Alkali resistance of selected waste fibres to model cement environment

Mrduljaš, Branka; Baričević, Ana; Pucić, Irina; Carević, Ivana; Didulica, Katarina

Case Studies in Construction Materials 19 (2023) e02411

Contents lists available at ScienceDirect

Case Studies in Construction Materials

journal homepage: www.elsevier.com/locate/cscm

Alkali resistance of selected waste fibres to model cement environment

Branka Mrduljaš [a], Ana Baričević [a,*], Irina Pucić [b], Ivana Carević [a], Katarina Didulica [a]

[a] University of Zagreb Faculty of Civil Engineering, Department of Materials, Fra Andrije Kačića Miošića 26, 10 000 Zagreb, Croatia
[b] Ruđer Bošković Institute, Division of Materials Chemistry, Bijenička 54, 10 000 Zagreb, Croatia

ARTICLE INFO

Keywords:
Production waste fibres
Recycled polymer fibres
Synthetic pore solution
Corrosion in cement

ABSTRACT

Synthetic fibres are often used to reinforce cementitious composites. However, their production has significant negative environmental impact. An ecological alternative could be to use waste fibre if their properties are found to be satisfactory. Therefore, the main objective of this study was to determine if selected waste fibres could withstand an aggressive and highly alkaline environment of cementitious composites. Three types of production waste fibres (alkali-resistant glass fibres, AR-GF, basalt fibres, BF and carbon fibres, CF and recycled tyre polymer fibres RTPF) were exposed to a synthetic pore solution simulating the cement matrix condition for 90 days. The mechanical properties of the production waste fibres and the morphology determined by scanning electron microscopy were the best predictors of fibre resistance. The sizing of the treated production waste fibres partially (CF) or completely (AR-GF, BF) decomposed. The pronounced deterioration of the BF structure was accompanied by a complete deterioration of the mechanical properties. A slight deterioration of mechanical properties was also observed in CF and to an even greater extent in AR-GF. The RTPFs were too short for mechanical measurements, so a combination of Fourier transform infrared spectroscopy and thermal analysis was required to evaluate effects of exposure to synthetic pore solution. The retained properties of treated RTPF seemed to be at least equivalent to those of AR-GF. Overall, the alkaline resistance of all studied waste and recycled tyre polymer fibres appears to be sufficient to restrain early age deformation of cementitious composite.

1. Introduction

High-quality synthetic fibres such as carbon fibres (CF), glass fibres (GF), or basalt fibres (BF) are widely used to reinforce cementitious materials, especially to reduce shrinkage and/or post-cracking [1–4]. Usually newly produced fibres are used despite enormous amounts of high-quality waste fibers, e.g., as leftovers from the technical textile industry or certain recycling processes. Considering the urgent need for the construction industry to make the transition from traditional to circular economy, it is imperative to reuse/recycle high value residual materials and stop further unnecessary consumption of raw materials. Newly produced synthetic fibres are subject to strict quality control requirements but after cutting and further processing, their properties may deteriorate posing a major challenge for reuse. Thus, this research focuses on four types of fibres that are either production waste (alkali-resistant glass -

* Correspondence to: University of Zagreb Faculty of Civil Engineering, Fra Andrije Kačića-Miošića 26, 10 000 Zagreb, Croatia.
E-mail address: ana.baricevic@grad.unizg.hr (A. Baričević).

https://doi.org/10.1016/j.cscm.2023.e02411
Received 21 April 2023; Received in revised form 14 August 2023; Accepted 17 August 2023
Available online 18 August 2023

AR-GF, basalt - BF, carbon fibres - CF) or a by-product of mechanical recycling of scrap tyres (recycled tyre polymer fibres, RTPF). To the best of the author's knowledge, this is the first study to analyse the selected end-of-life fibres under a synthetic pore solution.

The peculiarity of cementitious composites is their high alkalinity (pH >12), which creates an aggressive environment. Considering that a production and/or recycling process can negatively affect fibre properties a detailed characterization is required. Current studies mostly focus on industrially produced fibres (Table 1), while studies on waste fibres are rare. Studies conducted on industrially produced fibres indicate that corrosion mechanisms of GF and BF [5,6] are similar and show they are particularly affected by a highly alkaline cement environment (pH > 12) [7]. Pure glass fibres (GF) decompose in the presence of acids [8] and alkalis [9]. Therefore, up to 15% by weight of ZrO_2 is added to obtain alkali-resistant glass fibres (AR-GF), but it is still not completely inert to the cementitious environment [10]. The residual properties of BF exposed to alkaline environment are lower than those of glass fibres [11], while the durability of carbon fibres (CF) is less well studied and the results are contradictory. Some of the studies state that CF does not corrode under alkaline conditions [12] and does not absorb moisture [13], while others find partial or complete degradation [14]. Studies on waste selected fibres are rare. Onuaguluchi et al. [15] reported some corrosion of recycled tyre polymer fibres in the form of a slight increase in roughness and pitting, i.e., the formation of larger voids on the fibre surface. However, it was not determined how these changes affected fibre properties. No other studies on the durability of selected production waste fibres were found. Currently, there is no standard protocol for determining the alkali resistance of fibres in cementitious environments. In an attempt to simulate the cementitious environment solutions of various chemical compositions are used (Table 1). The most commonly used are saturated solutions of $Ca(OH)_2$ or NaOH [12,16] to which some authors added KOH and/or NaCl [17,18], but in the latter case the pH does not adequately mimic the alkalinity of a high-quality concrete [19]. Treatment conditions, such as the duration of fiber immersion and solution temperature also vary. Since the corrosion mechanism and its kinetics are affected by all those parameters [20], it is impossible to compare the results of different researcher's groups. Studies on the durability of fibres in the real cement environment are also scarce. Few researchers have studied the durability of glass or basalt fibres in cement solutions [5,21], and some even in the cement matrix [9,10]. Because the experiments in the cement matrix are time consuming, accelerated test methods in solutions may provide sufficient information on fibre durability in spite of their limitations. Taking all that in consideration a synthetic pore solution proposed by Poursaee [20] was selected as model for an alkaline environment for this study. That synthetic pore solution is prepared by combining $Ca(OH)_2$, NaOH, KOH, $CaSO_4 \times H_2O$ what is important because two types silicate-based fibre corrosion mechanisms are distinguished [21]. In saturated $Ca(OH)_2$ solution, corrosion starts at the initial cracks and flaws of the fibres and then slowly decomposes the structure, while the fibre diameter does not change significantly. However, the real cementitious pore solution contains other ions that play a role in the corrosion processes, especially Na^+ and K^+. In their presence, a porous gel is formed on the fibre surface, which facilitates the transport of water and alkalis and accelerates the dissolution of the silicate-based fibre. The fibre under the porous gel layer remains intact, but its residual diameter decreases.

To evaluate the most important fibre properties and those most affected by the alkaline treatment, characterization methods were selected such as mechanical properties and morphology. Some spectroscopic methods and thermal analysis were added to detect structural changes in the fibres exposed to the synthetic pore solution. If this study proves that waste fibres are resistant to the highly alkaline environment of cementitious composites the most important requirement for their future use in reinforcement of cementitious composites would be met.

Table 1
Exposure conditions testing alkaline resistance of synthetic fibres.

Type of fibres	Solution			Exposure time	References
	Type	pH value	Temperature		
Industrially produced fibres					
AR GF, BF, CF	NaOH	pH ≈ 13.0 – 14.0	22 °C ± 3°, 20, 40, 60, 80 & 100°C, Cooked	from 2 h up to 4 months	[5,6,12,16,18, 21-29]
	$Ca(OH)_2$	pH= 12.6	23 ± 2°C, 20 and 45 °C, 80°C	From 1 day up to 1 year	[12,17,18,25,29, 30]
	KOH	pH 12.7 & 14.0	20, 45 °C & 80°C	1–180 days	[12,17,25,29]
	NaOH + KOH + $Ca(OH)_2$	pH= 12.5	23°C	28, 90 and 180 days	[12,16]
AR GF, BF	Cement solution	pH≈ 13.0 – 14.0	23 ± 2°C, 80°C	From 6 h up to 4 months	[5,21,31]
AR GF	NaOH + KOH	pH= 13.50	50°C	up to 180 days	[32]
BF	NH_3	-	-	90 days	[29]
	Na_2SO_4	pH= 9.22	Room temperature	3–62 days	[18,28]
	NaOH+ Na_2SO_4	pH= 12.90	-	3–62 days	[18,28]
	NaOH and HCl		100°C	0,5 – 3 h	[27]
	NaOH+ NaCl	pH= 12.80–12.84	-	3–62 days	[18,28]
	NaOH+NaCl+Na_2SO_4	pH= 13.35	-	3–62 days	[18,28]
AR GF, BF	Cement matrix	-	20 ± 3°C, 55 °C	from 28 days up to 1 year	[9,10,33,34,35]
Waste fibres					
RTPF	NaOH + $Ca(OH)_2$ +NaCl)	13.0	20, 40, 60 & 80°C	3 months	[15]

2. Materials and methods

2.1. Fibres

Alkali-resistant glass (AR-GF), basalt (BF), carbon (CF) waste fibres were obtained from the textile manufacturer Kelteks Ltd, Karlovac, Croatia. The properties of these inorganic fibres as described in the technical data sheets [36–38] are listed in Table 2. The AR-GF, BF and CF are coated with several nanometers thick sizing to protect the fibre surface and improve its interphase properties [39]. According to the technical data sheets sizing of AR-GF and BF fibres is silane-based, while CF is protected by a polyurethane-based sizing [36–38].

The recycled tyre polymer fibres (RTPF) were obtained from Gumiimpex - GRP Ltd, Varaždin, Croatia. As a consequence of tire recycling process RTPF contains an unknown amount of fine rubber particles that cannot be completely removed. The fibre composition of RTPFs is known from previous studies [40]. RTPFs are short (average length of 8 mm) and exhibit high length variability, with a coefficient of variability of 58%, Table 2.

The production waste fibres (AR-GF, BF, CF) were cut to a length of 50 mm, while the RTPF were used as received. The samples were dried in an oven at 50 ± 2 °C for 48 h and then cooled in a desiccator on anhydrous calcium oxide at room temperature for 5 h [41].

All fibres used in this study belong to the category of microfibres (d < 0.3 mm) [42].

2.2. Synthetic pore solution

The synthetic pore solution used in this study was prepared based according to that used by Poursaee [20] and it consisted of 2.2 g/L $Ca(OH)_2$, 3.99 g/L NaOH, 16.83 g/L KOH, 0.34 g/L $CaSO_4 \times H_2O$ dissolved in distilled water. The fibre samples were immersed for a period of 90 days. The pH of the solution was monitored weekly using a laboratory pH meter with automatic sensor recognition, SI Analytics, Lab 850. The pH fluctuated slightly, with an average value of pH = 13.62 ± 0.33. To remove the soluble part of the precipitate, treated samples were heated in a steam bath at 40 °C for 1 h. The samples were removed from the steam bath, washed with distilled water and drained on the filter paper and then dried in an oven at 50 ± 2 °C for 48 h. After cooling to room temperature in a desiccator on anhydrous calcium oxide, the mass (m_{90}) was determined.

2.3. Characterization methods

The fibre diameter was determined on 100 fibres per fibre type using the projection microscope method according to EN ISO 137:2015 [42].

The solubility of the fibres was determined as the total mass loss after exposure to the synthetic pore solution. It was expressed as the percentage difference between the initial mass, $m_{0,}$ and the mass of the washed and dried samples after 90 days of immersion, m_{90}. Mass loss was calculated using the following equation:

$$\text{Mass } loss(\%) = \left(\frac{m_0 - m_{90}}{m_o}\right) x100 \quad (1)$$

where: m_0 = dry mass before treatment (g), m_{90} = dry mass after 90 days of immersion, respectively (g).

The tensile strength and modulus of elasticity of production waste fibres were measured using Vibroscope & Vibrodyn 400, Lenzing instruments, on 50 mm long specimens according to ISO 5079:2020 [43]. A single fibre was clamped with clamps having a gauge length of 20 mm, subjected to a preload, and then stretched at a constant rate of 10 mm/min until it cracked. The breaking force and

Table 2
Properties of fibres before and after the exposure to synthetic pore solution.

Fibre type	AR-GF	BF	CF	RTPF
Before the treatment				
Number of filaments (yarn)*	1 500	1 000	47,000	-
Density (g/cm^3) *	2.68	2.67	1.77	0.96 – 1.16
Linear density (tex) *	1 200	600	3 200	-
Sizing (%, type) *	0.80 (aminosilane)	> 0.40 (silane)	0.95–1.45 (PU)	-
Diameter (μm)	20.4 ± 2.4	17.2 ± 2.1	7.1 ± 1.0	18.0 ± 5.1
Length (mm)	50	50	50	1,0 – 28,0
Tensile strength (MPa)	1849 ± 72	2063 ± 104	828 ± 73	n/a
Modulus of elasticity (GPa)	61 ± 2.4	67 ± 3.4	133 ± 12	n/a
After the treatment				
Solubility/Mass loss (%)	25	32	4.4	n/a
Diameter (μm)	19.3 ± 5.5	17.0 ± 2.0	7.1 ± 1.0	19.8 ± 5.8
Tensile strength (MPa)	481 ± 78	13.4 ± 0	574 ± 77	n/a
Modulus of elasticity (GPa)	39 ± 6.3	n/a	115 ± 15	n/a

*Data from technical data sheets given by producer

breaking strain were recorded for 50 fibres of each type and for another 50 fibres after exposure to synthetic pore solution in order to determine residual mechanical properties. Since RTPFs were shorter than the gauge length of the instrument, their tensile strength and elastic modulus could not be determined.

The surface morphology of the fibres was studied by scanning electron microscopy (SEM) using Mira II LMU Tescan FE-SEM. Fibre samples were evaporated and then coated with a chromium layer.

Attenuated total reflection Fourier transform infrared spectra (ATR-FTIR) were recorded using the Bruker Tensor II instrument with diamond ATR in the frequency range 4000–400 cm^{-1}. No sample preparation was required. Spectra were processed using Spectragryph™ software.

Thermal analysis included thermogravimetric analysis (TG) of all fibre samples and differential scanning calorimetry (DSC) of RTPF. TG was performed using a TGA 55 instrument, TA Instruments. Approximately 5 mg of a fibre sample was placed in a platinum pan and equilibrated at 30 °C for 20 min prior to measurement. The mass change was recorded over a temperature range of 30–1000 °C at a rate of 10 °C per minute under a nitrogen atmosphere. DSC thermograms were recorded under nitrogen atmosphere on a Pyris device Diamond Perkin Elmer DSC. About to 5 mg of a sample was weighted with a precision of 0.1 mg, placed in an aluminium sample and crimped. Two heating and cooling cycles were performed under nitrogen atmosphere in the temperature range between 50 °C and 300 °C at a rate of 20 °C/min. DSC thermograms of least two samples of untreated and treated RTPF were recorded.

3. Results and discussion

The 90 days of fibre exposure to a synthetic pore solution corresponds to the period in which most of the (undesirable) changes occur in a real cement matrix. Before the exposure, the surface of the production waste fibres (AR-GF, BF, CF) was shiny with a distinctive colour (Fig. 1). After the alkaline treatment, the texture changed, the colour faded, and there was no gloss. The most noticeable changes occurred in BF, which became fragmented, consistent with observations from previous studies [18,28].

The RTPFs were initially of varying length, loose and contained rubber particles. Unlike the production waste fibres, the treated RTPFs appeared to be purified, as some of the rubber particles were washed out.

Overall mass loss (Table 2) of BF greater than 30% indicates the highest solubility of all fibres studied. Similar results were obtained by *Afroz* et al. [18], who treated both unsized and silane-sized BF in pure $Ca(OH)_2$ solution for 62 days. The solubility of the studied AR-GF was lower than that of BF but also significant, while *Ramachandran* et al. [24] found that the resistance of BF and AR-GF was similar but in NaOH solution. The mass loss of CF was low and the lowest among all the production waste fibres studied. On the other hand, mass loss is not a reliable indicator of the solubility of RTPF fibres because an unknown portion of initially present rubber particles was washed out during the alkali treatment.

After synthetic pore solution treatment, the diameter of AR-GF and BF was marginally reduced, by less than 5% (Table 2), which is consistent with the corrosion mechanism involving gel formation [21]. The diameter of CF remained unchanged while the diameter of RTPF increased by 10%, indicating swelling of the organic polymer fibres (Table 2).

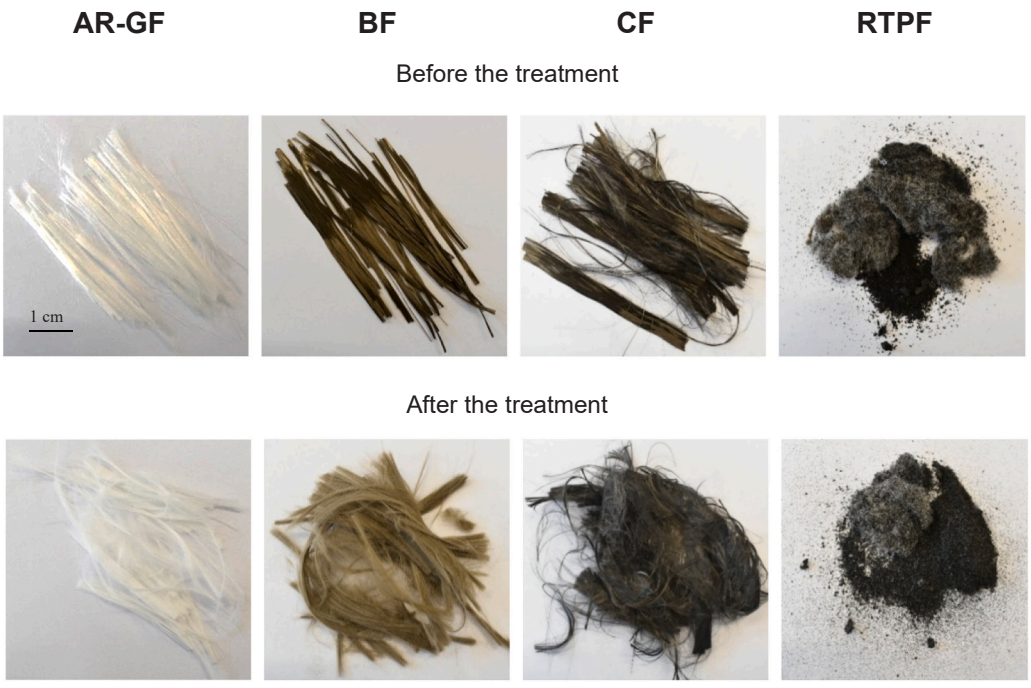

Fig. 1. Appearance of studied fibres before and after the alkali treatment.

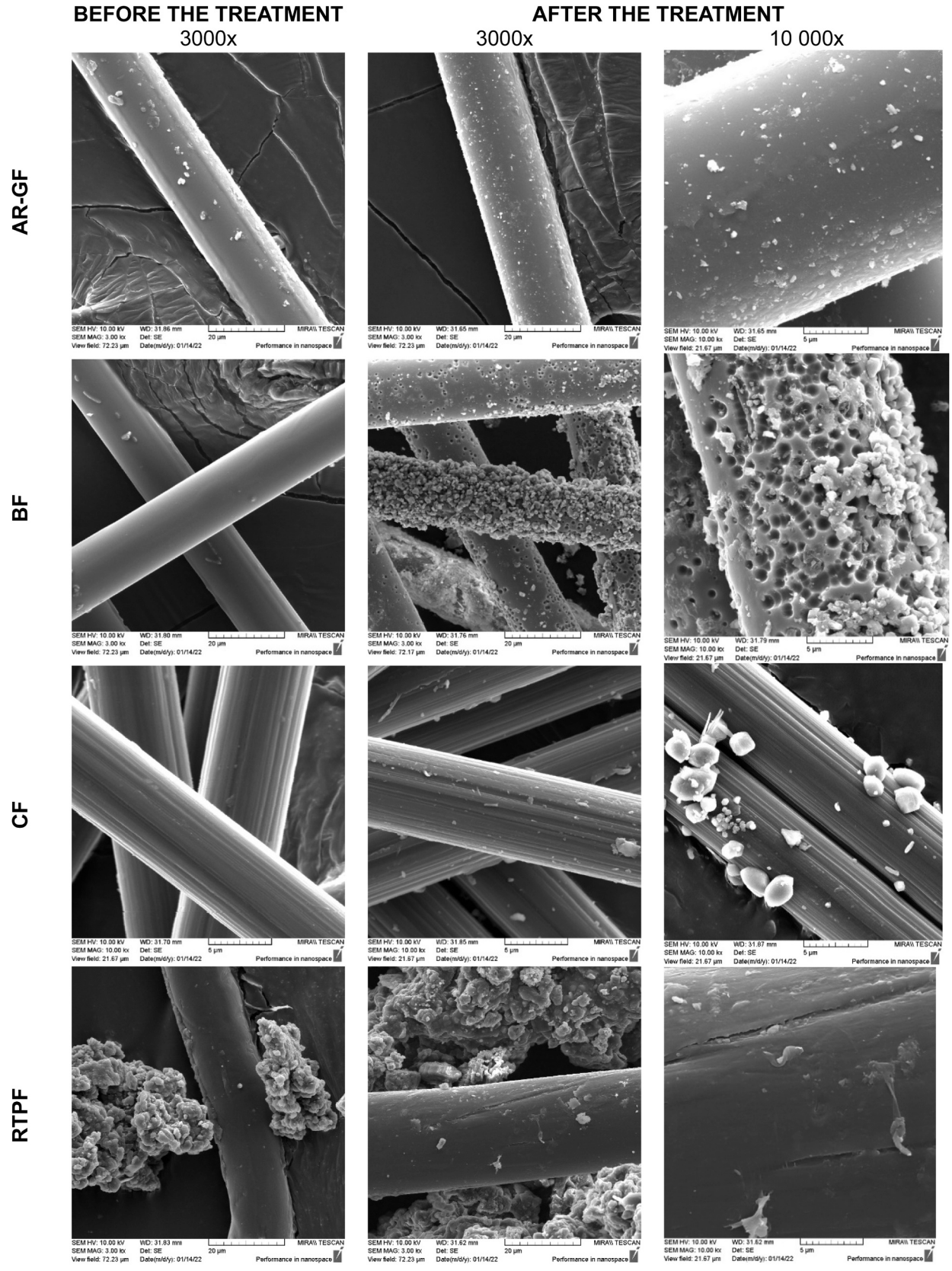

(caption on next page)

Fig. 2. SEM micrographies of the fibre surface, before (left column) and after the exposure to synthetic pore solution. Type of fibre and magnification is indicated in the figure.

Initial tensile strength of BF was the highest of all untreated production waste fibres, while the highest modulus of elasticity was that of untreated CF (Table 2) [44]. Exposure to synthetic pore solution resulted in a significant decrease in the average tensile strength and modulus of elasticity of all production waste fibres. Fibre type affected the outcome and resulted in a decreasing order of the tensile

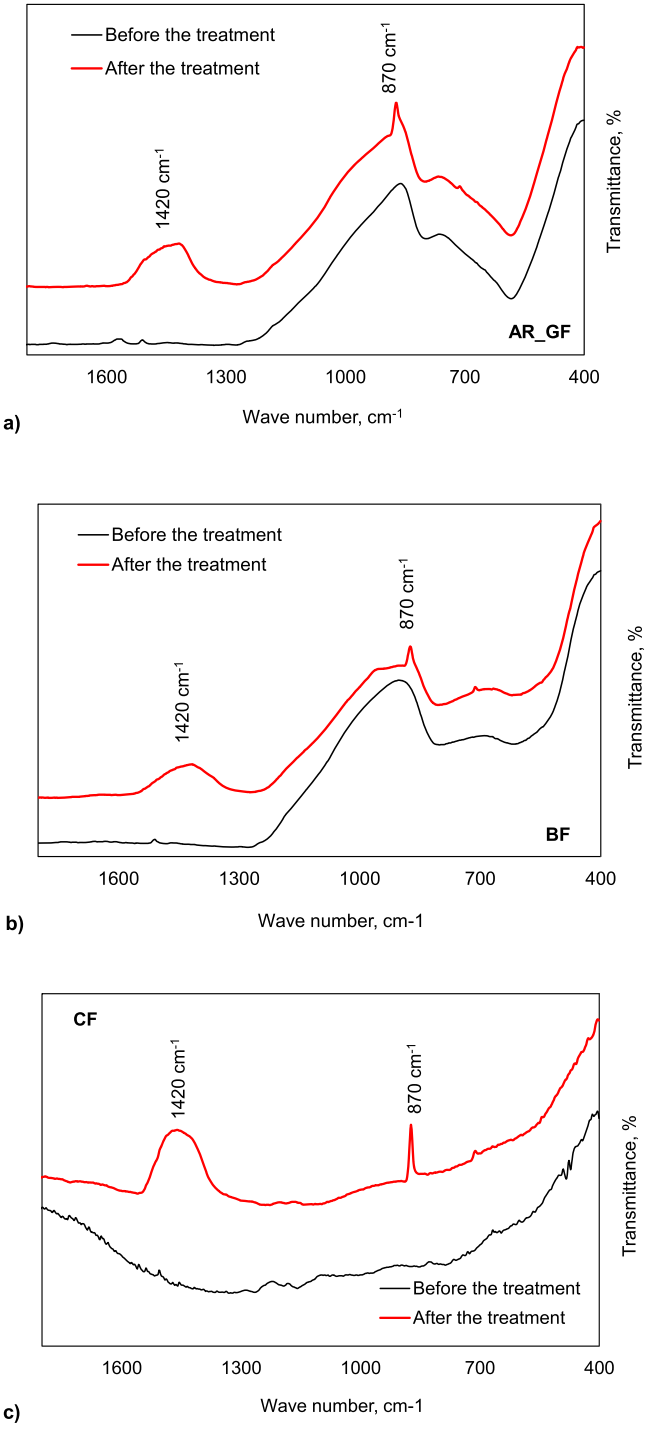

Fig. 3. a) ATR-FTIR spectra of production waste fibres before (black lines) and after the alkali treatment (red lines): a) AR-GF; b) BF; c) CF.

strength: CF, AR-GF, BF. While the tensile strength of CF decreased about 30%, that of AR-GF almost 75%, the tensile strength of the treated BF decreased below the pretensioning force of 13.4 MPa, causing the fibres to break during prestressing and made it impossible to determine BF's elastic modulus. The elastic moduli of treated production waste fibres followed the same trend as the tensile strength. Overall, the mechanical properties of CF were best preserved. As already mentioned, the mechanical properties of RTPF could not be evaluated because the fibres were too short.

Previous studies [45,46] have shown that the surface morphology of fibers is in a part influenced by the nature of the protective sizing. The individual "particles" on the surface of untreated production waste fibers revealed in SEM micrographies (Fig. 2, left column) are likely due to non-uniform coating of the sizing [30,44]. The surface of untreated AR-GF and BF was smooth, while grooves were visible on the surface of untreated CF. These grooves are intentionally created, to increase friction at the fibre/matrix interface and improve load transfer in fibre-reinforced composites [45].

SEM micrographs of alkali-treated production waste fibers (AR-GF, BF, CF) showed varying degrees of sizing decomposition and precipitate formation. According to *Wang* et al. [21], a crucial step in the silicate fibers (BF and AR-GF) corrosion is an attack of hydroxyl ion (OH^-) and breaking of the Si-O-Si bond, which causes the silicates to migrate into the solution. The greatest damage, including pitting, was observed on the surface of the basalt fibers that are slightly less dense than AR-GF [27]. Such changes have already been observed by other researchers [18]. In addition, the largest amount of precipitate formed on the surface of BF.

The untreated RTPF (Fig. 2, bottom left) contained significant quantities of rubber particles. Fibre surface was rough and localized damage was visible, most likely caused by the mechanical recycling process of scrap tires. On the fiber surface of alkali treated RTPF additional cracks were observed on the fiber surface and there were almost no rubber particles present (Fig. 2 bottom, middle and right).

ATR-FTIR spectra (Fig. 3) of untreated production waste fibres appear to be relatively featureless apart from a broad silicate absorption with a maximum at about 900 cm^{-1} in AR-GF and BF. Closer examination of the spectra of AR-GF and BF revealed very weak absorptions of amino groups between 1600 and 1500 cm^{-1}. These absorptions suggest that the sizing may be an organic amino-silane. Polyurethane absorptions of the proposed CF sizing were not observed.

Two additional strong maxima were observed in the spectra of all the treated production waste fibres (AR-GF, BF and CF): a broad one at 1420 cm^{-1} and a sharp one at 870 cm^{-1}. These two maxima are characteristic of carbonate ions and indicate that the precipitate

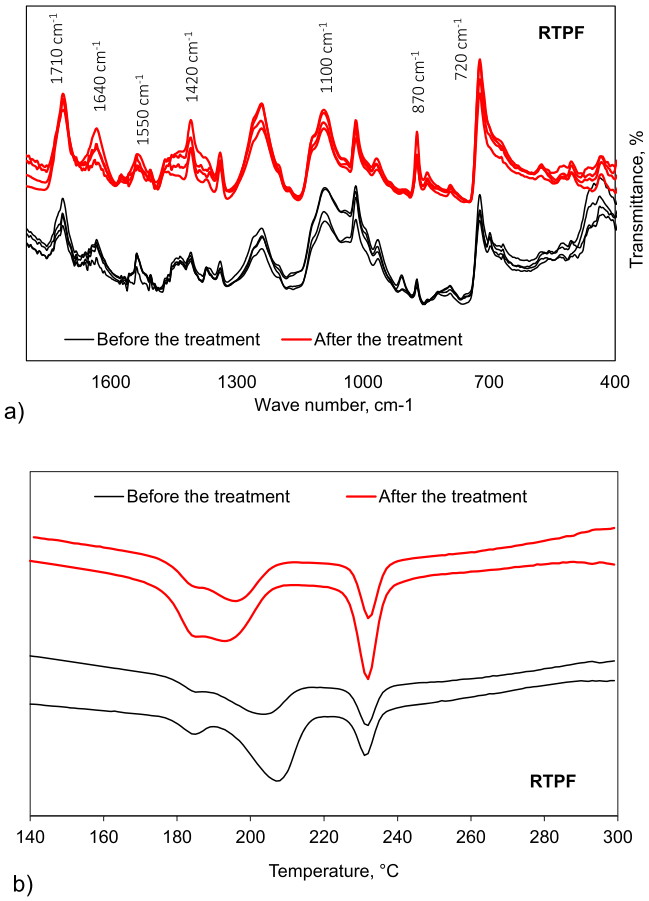

Fig. 4. RTPF fibres before (black lines) and after the alkali treatment (red lines); a) ATR-FTIR spectra recorded on a several locations, b) DSC cooling thermograms of 2 samples of untreated (black lines) and 2 samples of treated RTPF (red lines).

deposited on the fibre surface is calcium carbonate [47]. Carbonate ions form when carbon dioxide is dissolved in an alkaline solution that has been in contact with air. Since calcium carbonate is poorly soluble in alkaline solutions, it deposited on the fibre surface. The formation of the deposits was independent of the chemical nature of the fibre or the sizing, so the same spectral maxima were recorded for all inorganic fibres.

The ATR-FTIR spectra (Fig. 4a) reveal that the fibres of RTPF are constituted of polyester and polyamide. Characteristic polyester absorptions include a broad carbonyl stretching peak at 1710 cm^{-1}, a peak at 1100 cm^{-1} caused by the ester bond stretching, and a maximum at 720 cm^{-1} originating from the out-of-plane bending of the terephthalic monomer benzene ring [48]. The absorption of amide I at about 1640 cm^{-1} and amide II at about 1550 cm^{-1} peaks are typical polyamide absorptions. In the spectrum of the treated RTPF, the intensities of all maxima are slightly higher because most of the rubber particles have been washed out. The main change is a relative increase in the intensity of the maximum at 720 cm^{-1} compared to other polyester absorptions at 1710 cm^{-1} and at 1100 cm^{-1}. This change is likely caused by the partial alkaline hydrolysis of the ester bonds as the first step in the decomposition polyester fibres [48]. The relative intensities of the polyamide absorptions remained the same, indicating that the polyamide fibres of the RTPF were not affected by the synthetic pore solution. Carbonate maxima at 870 cm^{-1} and at 1420 cm^{-1} are also present in the spectra of the treated RTPF, confirming that some calcium carbonate precipitated on RTPF, likewise.

To confirm the FTIR findings that the polyester in treated RTPF only partial decomposes, differential scanning calorimetry (DSC) measurements were performed. An advantage of DSC is that, if an upper limit of the temperature range is below decomposition temperature, both melting and crystallization of thermoplastic polymers can be monitored. Since polyamides and polyesters such as PET and PBT are thermoplastic, DSC thermograms are useful in distinguishing the effects of synthetic pore solution treatment on each of the polymers constituting the RTPF. While the melting temperatures of polyesters and PA partially overlap, the crystallization temperatures are separated. In the DSC thermograms recorded during cooling (Fig. 4b). PA crystallizes at higher temperature, 235 °C while lower temperature crystallization peak consists of two partially merged minima. This is a consequence of the fact that PET and PBT are chemically and structurally similar and therefore crystallize at very similar temperatures, between 190 and 205 °C. Degradation increases the distribution of polymer chain size, which contributes to the broadening of the DSC peaks and the appearance of shoulders. As can be seen from the red thermograms of the treated RTPF (Fig. 4b), only the peak of polyester crystallization at lower temperature was affected, while the crystallization peak of PA was as sharp as in the untreated RTPF. The peak areas are proportional to the enthalpy of crystallization and the relative amount of a particular polymer in a mixture. Partial alkaline hydrolysis of the polyester component resulted in a relative decrease in polyester peak area and a relative increase in PA peak area, confirming the FTIR

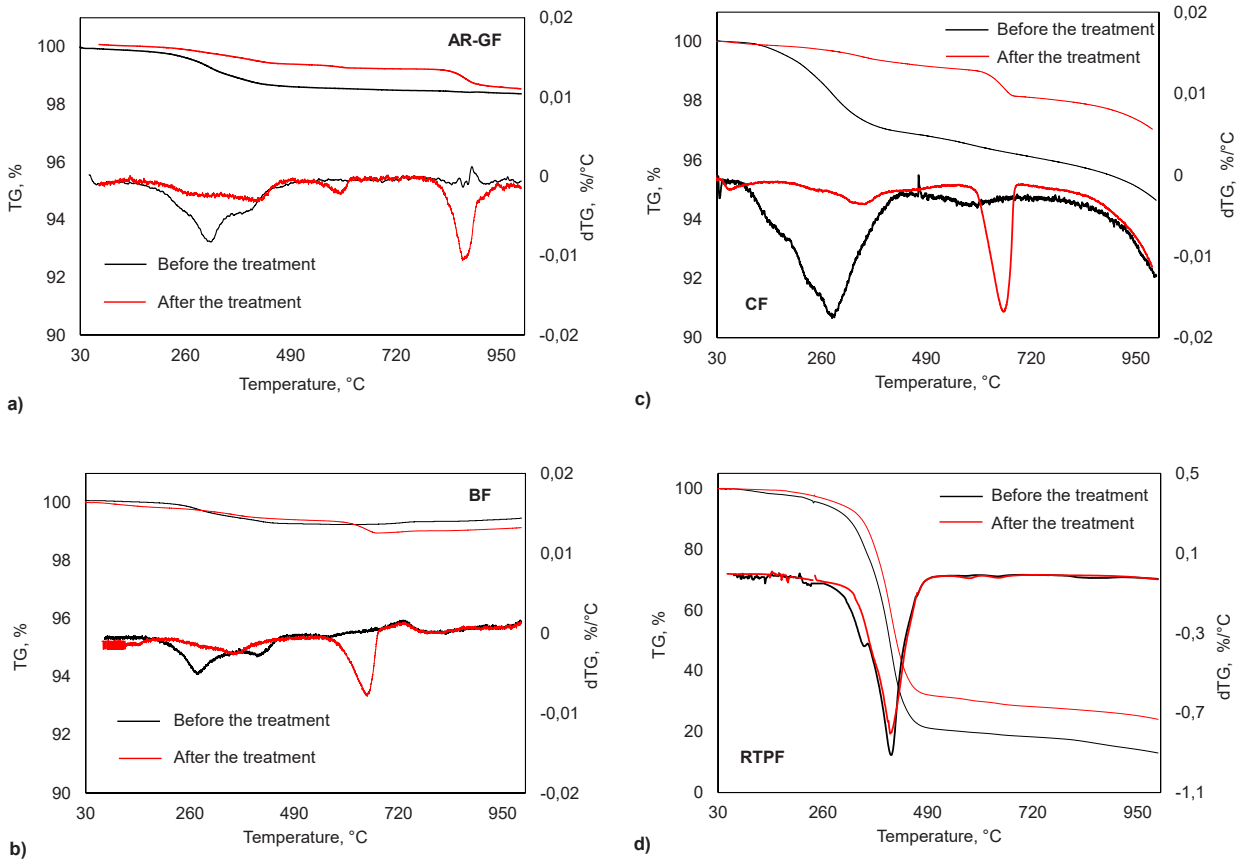

Fig. 5. TG and dTG curves of fibres before (black lines) and after (red lines) the alkali treatment: a) AR-GF, b) BF, c) CF, d) RTPF.

results. The transformation of calcium carbonate precipitates is at the temperatures well above the temperature range appropriate for polymer fibre analysis.

The thermal stability of the production waste fibres up to 1000 °C, as determined by thermogravimetry (TG), was very high (Fig. 5, a, b, c). The total mass losses of the untreated AR-GF and BF fibres were less than 3%, which corresponds to the amount of sizing reported in the technical data sheets. Indeed, the differential thermograms (dTG) of all the untreated production waste fibres reveal a peak mass loss at about 260 °C, which corresponds to the decomposition of the silane-based sizing [16]. In the case of the untreated CF, the mass loss was slightly higher (below 5%) up to 1000 °C, indicating that a larger amount of sizing was applied. However, in the dTG thermograms of CF there is no peak at about 400 °C that would confirm that it was coated with polyurethane. Instead, there is a peak in mass loss at about 260 °C as in dTG thermograms of AR-GF and BF. Thus, it appears that CF was also sized with amino-silane despite of manufacturer's claims. In the thermograms of BF, a very small mass increase was observed at temperatures above 600 °C, which is known to be due to reactions of the fibres with the nitrogen atmosphere [49]. The overall mass decrease of AR-GF and BF treated with synthetic pore solution up to 1000 °C was approximately the same as that of the corresponding untreated fibres. In the differential thermograms of the treated AR-GF and BF, there was no peak at 260 °C, confirming that the sizing was dissolved. In the dTG thermograms of the treated CF there was still a smaller peak corresponding to traces of sizing, probably because more sizing had been initially applied. In the thermograms of all treated production waste fibres, there was a new mass loss at higher temperature, between 600 and 800 °C. Since $CaCO_3$ decomposes in this temperature range [50], the new mass loss is apparently due to the decomposition of calcium precipitates formed on the fibre surface. Overall, the treated production waste fibres appear to be as stable below 1000 ºC as the untreated fibres.

Since RTPF is mainly composed of organic polymers, about 88% of its total mass decomposed in the temperature range below 500 °C (Fig. 5d). Thermal decomposition of PET and PA 66 constituents of RTPF are seen as dTG peaks at about 400 °C, and when more PBT was present, a shoulder appeared at 340 °C. The thermal stability of treated RTPF was the same as that of untreated. There is no mass loss in thermograms of treated RTPF that could be attributed to the decomposition of $CaCO_3$. Since the mass loss of RTPF is about two orders of magnitude greater than that of production waste fibres, the decomposition of the precipitate is too insignificant to be observed. The differences in the final residual mass of the untreated and treated RTPF are due to various amounts of impurities present.

The fibres can provide their function in cementitious composites only if mechanical properties are preserved enough. Sizing seems to contribute a lot to the average tensile strength of a fibre, for example Yang and Thomason found that in case of E – glass fibre it was between 40% and 80% [51]. Thus, reduction of tensile strength of AR-GF and BF fibres after exposure to a synthetic pore solution can be partially explained by the loss of sizing. However, the change in mechanical properties of studied fibres was found to be primarily dependent on fibre composition. Particularly noticeable was the deterioration of initially toughest fibre, BF. The complete degradation of the sizing of AR-GF and BF fully exposed their surface defects. According to *Scheffler* et al. [5] it leads to stress concentration at the tip of the cracks and then corrosion progresses to pitting and failure at reduced stress levels. Such a detrimental decomposition mechanism occurred particularly in BF that became severely corroded and difficult to handle and test. SEM micrographies revealed pitting therefore such morphology changes are a good indicator of significant corrosion. Although both AR-GF and BF are chemically similar, composed of SiO_2 and Al_2O_3, AR-GF retained about a quarter of its initial tensile strength. The backbone of glass fibres is denser than that of basalt ones [27], and a Zr_2O layer acts as a barrier that further reduces the corrosion rate so that the breaking of the Si-O-Si network under the attack of hydroxyl ions is slower. The high carbon content (over 90%) and an amorphous structure of CF, give these fibres both high tensile strength and excellent chemical resistance [12,52] that depended much less on the stability of sizing. A slight deterioration of the mechanical properties is likely a consequence of the accumulation of calcium precipitates on the fibre surface.

Assessment of the alkaline resistance of short fibres like RTPF posed a new set of problems because mechanical measurements could not be performed and impurity washout in the synthetic pore solution made mass loss an inappropriate method to determine solubility. Therefore, predictions of RTPF behaviour in cementitious composites had to be made based on the results of the methods such as FTIR and DSC. The results showed that alkaline hydrolysis occurred only partially and affected only the polyester part of the RTPF while polyamide fibres were stable. It is consistent with SEM findings that the number of defects increased just slightly. Thus, it can be proposed that RTPF are also resistant enough to at least prevent early age cracking of cementitious composites.

4. Conclusions

The resistance of production waste fibres to a synthetic pore solution as a model for a cementitious environment was similar to that of regular industrial fibres of corresponding chemical composition. Carbon fibres (CF) were the most stable to 90 days of alkaline exposure while basalt fibres (BF) were the least stable and completely lost their otherwise very high tensile strength. Sizing, the protective layer, contributed to the stability of the alkali-resistant glass (AR-GF). Nevertheless, the resistance of all production waste fibres appears to be sufficient to restrain crack development and early age deformation of cementitious composite, thus preserving at least one of the functions of the fibres in the cement matrix.

Residual mechanical properties and preserved morphology are the best predictors of fibre behaviour in a cement composite. The RTPF were too short for mechanical measurements, but other methods revealed only partial and limited alkaline hydrolysis. Thus, it can be predicted that the durability of RTPF is at least as good as that of AR-GF, suggesting that they can also be used to at least limit early age volume deformation.

The differences in composition and properties between production waste fibres and RTPF highlight the difficulty of establishing standardized testing protocols. These protocols should include established physical and chemical methods that can be used to evaluate the relevant properties of various waste fibre types. In this way, the circular economy would be promoted.

Further research should focus on correlating the results of accelerated test methods with the actual rate of degradation of fibres in cementitious composites. Therefore, standardisation of test methods, model solutions, and conditions for accelerated ageing of textile fibres would facilitate these correlations.

Funding

The research presented here was carried out as part of the projects "Cement Composites Reinforced with Waste Fibers" - ReWire (UIP-2020-02-5242) and "Young Researchers' Career Development Project - Training New Doctoral Students" (DOK-2021-02-4884) at the University of Zagreb Faculty of Civil Engineering, both funded by the Croatian Science Foundation.

CRediT authorship contribution statement

B. Mrduljaš: Formal analysis, Investigation, Data curation, Writing – original draft. **A. Baričević:** Conceptualization, Methodology, Formal analysis, Writing – original draft, Funding acquisition, Supervision. **I. Pucić:** Data Curation and Formal analysis, Writing – review & editing, Supervision, Validation. **I. Carević:** Formal analysis, Writing – review & editing. **K. Didulica:** Investigation, Data curation.

Declaration of Competing Interest

The authors declare that they have no competing financial interests or personal relationships that could have appeared to influence the work reported in this paper.

Data Availability

Data will be made available on request.

Acknowledgements

The authors would like to thank Dr. Friedrich Menges for the free use of his spectroscopy software SpectragryphTM (Menges, 2019). Special thanks to Kelteks Ltd., Karlovac, Croatia (www.kelteks.com) and Gumiipex – GRP d.o.o. (www.gumiimpex.com) for providing resources and continuous support in the implementation of the ReWire project.

References

[1] A. Baričević, M. Jelčić Rukavina, M. Pezer, N. Štirmer, Influence of recycled tire polymer fibers on concrete properties, Cem. Concr. Compos. vol. 91 (2018) 29–41, https://doi.org/10.1016/j.cemconcomp.2018.04.009.
[2] F.A. Mirza, P. Soroushian, Effects of alkali-resistant glass fiber reinforcement on crack and temperature resistance of lightweight concrete, Cem. Concr. Compos. vol. 24 (2) (2002) 223–227, https://doi.org/10.1016/S0958-9465(01)00038-5.
[3] V. Fiore, T. Scalici, G. Di Bella, A. Valenza, A review on basalt fibre and its composites, Compos. Part B Eng. vol. 74 (2015) 74–94, https://doi.org/10.1016/j.compositesb.2014.12.034.
[4] A.M. Brandt, Fibre reinforced cement-based (FRC) composites after over 40 years of development in building and civil engineering, Compos. Struct. vol. 86 (1–3) (2008) 3–9, https://doi.org/10.1016/j.compstruct.2008.03.006.
[5] C. Scheffler, T. Förster, E. Mäder, G. Heinrich, S. Hempel, V. Mechtcherine, Aging of alkali-resistant glass and basalt fibers in alkaline solutions: evaluation of the failure stress by Weibull distribution function, J. Non Cryst. Solids vol. 355 (52–54) (2009) 2588–2595, https://doi.org/10.1016/j.jnoncrysol.2009.09.018.
[6] M. Friedrich, et al., Investigation of chemically treated basalt and glass fibres, Mikrochim. Acta vol. 133 (1–4) (2000) 171–174, https://doi.org/10.1007/s006040070088.
[7] A. Mohajerani, et al., Amazing types, properties, and applications of fibres in construction materials, Materials vol. 12 (16) (2019) 1–45, https://doi.org/10.3390/ma12162513.
[8] F. Fourné, Synthetic Fibers: Machines and Equipment, Manufacture, Properties, 1st ed., vol. 59, no. 7. Hanser Publications, 1999.
[9] V.T. Yilmaz, Chemical attack on alkali-resistant glass fibres in a hydrating cement matrix: characterization of corrosion products, J. Non Cryst. Solids vol. 151 (3) (1992) 236–244, https://doi.org/10.1016/0022-3093(92)90035-I.
[10] B. Holubová, H. Hradecká, M. Netušilová, T. Gavenda, A. Helebrant, Corrosion of glass fibres in ultra high performance concrete and normal strength concrete, Ceram. - Silik. vol. 61 (4) (2017) 319–326, https://doi.org/10.13168/cs.2017.0031.
[11] A. Coricciati, P. Corvaglia, and G. Mosheyev, Durability of fibers in aggressive alkaline environment, Mater. Sci., no. January 2009, 2009, [Online]. Available: ⟨https://www.researchgate.net/publication/289835802⟩.
[12] F. Micelli, M.A. Aiello, Residual tensile strength of dry and impregnated reinforcement fibres after exposure to alkaline environments, Compos. Part B Eng. vol. 159 (2019) 490–501, https://doi.org/10.1016/j.compositesb.2017.03.005.
[13] A. Spelter, S. Bergmann, J. Bielak, J. Hegger, Long-term durability of carbon-reinforced concrete: an overview and experimental investigations, Appl. Sci. vol. 9 (8) (2019), https://doi.org/10.3390/app9081651.
[14] L.C. Bank, T.R. Gentry, A. Barkatt, Accelerated test methods to determine the long-term behavior of frp composite structures: environmental effects, J. Reinf. Plast. Compos. vol. 14 (6) (1995) 559–587, https://doi.org/10.1177/073168449501400602.
[15] O. Onuaguluchi, N. Banthia, Durability performance of polymeric scrap tire fibers and its reinforced cement mortar, Mater. Struct. Constr. vol. 50 (2) (2017), https://doi.org/10.1617/s11527-017-1025-7.
[16] S.L. Gao, E. Mäder, A. Abdkader, P. Offermann, Sizings on alkali-resistant glass fibers: environmental effects on mechanical properties, Langmuir vol. 19 (6) (2003) 2496–2506, https://doi.org/10.1021/la020778t.
[17] A. Helebrant, H. Hradecká, B. Holubová, L. Brázda, M. Netušilová, Z. Zlámalová-Cílová, Kinetics of processes modeling corrosion of glass fibre mixed nto concrete, Ceram. -Silikáty 61 (2) (2017) 163–171, https://doi.org/10.13168/CS.2017.0012.
[18] M. Afroz, I. Patnaikuni, S. Venkatesan, Chemical durability and performance of modified basalt fiber in concrete medium, Constr. Build. Mater. vol. 154 (2017) 191–203, https://doi.org/10.1016/j.conbuildmat.2017.07.153.

[19] Y. Sumra, S. Payam, I. Zainah, The pH of cement-based materials: a review, J. Wuhan. Univ. Technol. Mater. Sci. Ed. vol. 35 (5) (2020) 908–924, https://doi.org/10.1007/s11595-020-2337-y.
[20] A. Poursaee, Corrosion of steel bars in saturated Ca(OH)2 and concrete pore solution, Concr. Res. Lett. vol. 1 (3) (2010) 90–97. https://www.challengejournal.com/index.php/cjcrl/article/view/105.
[21] Q. Wang, Y. Ding, N. Randl, Investigation on the alkali resistance of basalt fiber and its textile in different alkaline environments, Constr. Build. Mater. vol. 272 (2021), 121670, https://doi.org/10.1016/j.conbuildmat.2020.121670.
[22] C. Tang, H. Jiang, X. Zhang, G. Li, J. Cui, Corrosion behavior and mechanism of basalt fibers in sodium hydroxide solution, Mater. (Basel) vol. 11 (8) (2018) 1–16, https://doi.org/10.3390/ma11081381.
[23] C. Scheffler, et al., Interphase modification of alkali-resistant glass fibres and carbon fibres for textile reinforced concrete I: Fibre properties and durability, Compos. Sci. Technol. vol. 69 (3–4) (2009) 531–538, https://doi.org/10.1016/j.compscitech.2008.11.027.
[24] B.E. Ramachandran, V. Velpari, N. Balasubramanian, Chemical durability studies on basalt fibres, J. Mater. Sci. vol. 16 (12) (1981) 3393–3397, https://doi.org/10.1007/BF00586301.
[25] M. Li, D. Xing, Q.Bin Zheng, H. Li, B. Hao, P.C. Ma, Variation on the morphology and tensile strength of basalt fiber processed in alkali solutions, Constr. Build. Mater. vol. 335 (January) (2022), 127512, https://doi.org/10.1016/j.conbuildmat.2022.127512.
[26] V.A. Rybin, A.V. Utkin, N.I. Baklanova, Alkali resistance, microstructural and mechanical performance of zirconia-coated basalt fibers, Cem. Concr. Res. vol. 53 (2013) 1–8, https://doi.org/10.1016/j.cemconres.2013.06.002.
[27] B. Wei, H. Cao, S. Song, Tensile behavior contrast of basalt and glass fibers after chemical treatment, Mater. Des. vol. 31 (9) (2010) 4244–4250, https://doi.org/10.1016/j.matdes.2010.04.009.
[28] H. Myadaraboina, D. Law, I. Patnaikuni, Durability of basalt fibers in concrete medium, Proc. Int. Struct. Eng. Constr. vol. 1 (1) (2014) 445–450, https://doi.org/10.14455/ISEC.res.2014.41.
[29] J.J. Lee, J. Song, H. Kim, Chemical stability of basalt fiber in alkaline solution, Fibers Polym. vol. 15 (11) (2014) 2329–2334, https://doi.org/10.1007/s12221-014-2329-7.
[30] M. Ryvolová, L. Svobodová, T. Bakalova, Validation of an image analysis method for evaluating the chemical resistance of glass fibers to alkaline environments, Materials vol. 15 (1) (2022), https://doi.org/10.3390/ma15010161.
[31] V. Velpari, B.E. Ramachandran, T.A. Bhaskaran, B.C. Pai, N. Balasubramanian, Alkali resistance of fibres in cement, J. Mater. Sci. vol. 15 (6) (1980) 1579–1584, https://doi.org/10.1007/BF00752141.
[32] J. Orlowsky, M. Raupach, H. Cuypers, J. Wastiels, Durability modelling of glass fibre reinforcement in cementitious environment, Mater. Struct. Constr. vol. 38 (276) (2005) 155–162, https://doi.org/10.1007/BF02479340.
[33] V. Pastsuk, et al., Selection of basalt fiber with resistance to concrete alkaline environment, SN Appl. Sci. vol. 2 (11) (2020) 1–17, https://doi.org/10.1007/s42452-020-03677-z.
[34] Y.V. Lipatov, S.I. Gutnikov, M.S. Manylov, E.S. Zhukovskaya, B.I. Lazoryak, High alkali-resistant basalt fiber for reinforcing concrete, Mater. Des. vol. 73 (2015) 60–66, https://doi.org/10.1016/j.matdes.2015.02.022.
[35] N. Arabi, L. Molez, D. Rangeard, Durability of alkali-resistant glass fibers reinforced cement composite: microstructural observations of degradation, Period. Polytech. Civ. Eng. vol. 62 (3) (2018), https://doi.org/10.3311/PPci.10631.
[36] O. Coring, CEM -FIL 5325 AR Direct Rowing." p. 10010692, 2014, [Online]. Available: ⟨https://www.owenscorning.com/en-us/composites/product/cem-filreinforcementfibers⟩.
[37] V. Kamenny, KV42 Assembled roving series." 2018, [Online]. Available: https://basfiber.com/.
[38] T. Carbon, Tenax FILAMENT YARN." 2020, [Online]. Available: https://www.teijincarbon.com/downloads.
[39] J.L. Thomason, Glass fibre sizing: a review, Compos. Part A Appl. Sci. Manuf. vol. 127 (September) (2019), https://doi.org/10.1016/j.compositesa.2019.105619.
[40] M. Serdar, A. Baričević, M. Jelčić Rukavina, M. Pezer, D. Bjegović, N. Štirmer, Shrinkage behaviour of fibre reinforced concrete with recycled tyre polymer fibres, Int. J. Polym. Sci. vol. 2015 (2015), https://doi.org/10.1155/2015/145918.
[41] A. Committee, ASTM D618–13, Standard Practice for Conditioning Plastics for Testing, vol. i. pp. 1–4, 2013, [Online]. Available: http://www.ansi.org.
[42] "ISO 137:2015 Wool – Determination of fibre diameter – Projection microscope method." p. 12.
[43] "ISO 5079:2020 Textile fibres — Determination of breaking force and elongation at break of individual fibres, p. 12.
[44] A. Baričević, K. Didulica, B. Mrduljaš, A. Ocelić, Production waste fibres as a sustainable alternative for strengthening cementitious composites, Int. RILEM Conf. Synerg. Expert. Towar. Sustain. Robust. Cem. Mater. Concr. Struct. (2023) 593–603, https://doi.org/10.1007/978-3-031-33211-1_53.
[45] M. Sharma, S. Gao, E. Mäder, H. Sharma, L.Y. Wei, J. Bijwe, Carbon fiber surfaces and composite interphases, Compos. Sci. Technol. vol. 102 (2014) 35–50, https://doi.org/10.1016/j.compscitech.2014.07.005.
[46] T. Yang, Y. Zhao, H. Liu, M. Sun, S. Xiong, Effect of sizing agents on surface properties of carbon fibers and interfacial adhesion of carbon fiber/bismaleimide composites, ACS Omega (2021), https://doi.org/10.1021/acsomega.1c01103.
[47] F.A. Andersen, L. Brečević, Infrared spectra of amorphous and crystalline calcium carbonate, Acta Chem. Scand. vol. 45 (1991) 1018–1024, https://doi.org/10.3891/acta.chem.scand.45-1018.
[48] R.M. Silverstein, F.X. Webster, and D.J. Kiemle, Spectrometric identification of organic compounds, 7th ed. 2005.
[49] M.A.G. Lazcano, Y. Weidong, Radiative and thermal characterization of basalt fabric as an alternative for firerighter protective clothing, Mater. Sci. vol. 10 (9) (2014) 371–376. https://www.tsijournals.com/abstract/radiative-and-thermal-characterization-of-basalt-fabric-as-an-alternative-for-firefighter-protective-clothing-4549.html.
[50] K. Scrivener, R. Snellings, and B. Lothenbach, A Practical Guide to Microstructural Analysis of Cementitious Materials. 2018.
[51] L. Yang, J.L. Thomason, Effect of silane coupling agent on mechanical performance of glass fibre, J. Mater. Sci. vol. 48 (5) (2013) 1947–1954, https://doi.org/10.1007/s10853-012-6960-7.
[52] J. Pusch, B. Wohlmann, Carbon Fibers, Chapter 2 in The Textile Institute Book Series, Inorganic and Composite Fibers, Editor(s): B. Mahltig, Y. Kyosev, Woodhead Publishing, Elsevier Ltd, 2018, https://doi.org/10.1016/B978-0-08-102228-3.00002-5.